

Ground state properties of a one-dimensional condensate of hard core bosons in a harmonic trap

M. D. Girardeau, E. M. Wright, and J.M. Triscari

Optical Sciences Center and Department of Physics

University of Arizona

Tucson, AZ 85721

(November 5, 2018)

Abstract

The exact N -particle ground state wave function for a one-dimensional condensate of hard core bosons in a harmonic trap is employed to obtain accurate numerical results for the one-particle density matrix, occupation number distribution of the natural orbitals, and momentum distribution. Our results show that the occupation of the lowest orbital varies as $N^{0.59}$, in contrast to $N^{0.5}$ for a spatially uniform system, and N for a true BEC.

03.75.Fi,03.75.-b,05.30.Jp

arXiv:cond-mat/0008480v2 [cond-mat.mes-hall] 31 Aug 2000

I. INTRODUCTION

Recent advances in atom de Broglie waveguide technology [1–5] and its potential applicability to atom interferometry [6] and integrated atom optics [3,7] create a need for accurate theoretical modelling of such systems in the low temperature, tight waveguide regime where transverse excitations are frozen out and the quantum dynamics becomes essentially one-dimensional (1D). It has been shown by Olshanii [8], and also recently by Petrov et al. [9], that at sufficiently low temperatures, densities and large positive scattering length, a Bose-Einstein condensate (BEC) in a thin cigar-shaped trap has dynamics which approach those of a 1D gas of hard core, or impenetrable, point bosons. This is a model for which the exact many-body energy eigensolutions were found in 1960 using an exact mapping from the Hilbert space of energy eigenstates of an *ideal* gas of fictitious spinless fermions to that of many-body eigenstates of hard core, and therefore *strongly interacting*, bosons [10,11]. In this limit there are strong short-range pair correlations which are omitted in the Gross-Pitaevskii (GP) approximation. In the absence of a trap potential it is known [12] that the occupation of the lowest orbital is of order \sqrt{N} where N is the total number of atoms, in contrast to N for the ideal Bose gas and GP approximation. Nevertheless, this system exhibits some BEC-like behavior such as Talbot recurrences following an optical lattice pulse [13] and dark soliton-like behavior in response to a phase-imprinting pulse [14].

The case of harmonically trapped, hard core bosons in 1D is more relevant to recent atom waveguide experiments [15]. The spatial density profile of the single-particle density is expressible in closed form, and has recently been shown [16] to be well approximated by a modified 1D effective field theory, although we have recently shown in a numerically accurate time-dependent calculation [17] that spatial interference of separated and recombined condensates is much weaker than that predicted by the corresponding time-dependent mean field theory [16]. Although the Fermi-Bose mapping theorem [10,11] implies that all physical properties expressible in terms of spatial configurational probabilities are the same for the actual bosonic system and the fictitious "spinless fermion" system used for the mapping, the momentum distribution of the bosonic system, or more generally its occupation distribution over the relevant orbitals for a given geometry, is very different in the bosonic system. It is known [8,12,18] that for a spatially uniform system of hard core bosons in 1D, the momentum distribution is strongly peaked in the neighborhood of zero momentum, whereas that of the corresponding Fermi system is merely a filled Fermi sea. In the case of hard core bosons in a 1D harmonic trap, it is an interesting and previously unanswered question whether the system undergoes true BEC or merely an attenuated one such as that in the uniform system. Ketterle and Van Druten [19] have shown that true BEC occurs for a finite number of atoms in a 1D harmonic oscillator (HO) for an ideal gas. We examine the question for hard core bosons in a 1D HO by using the Fermi-Bose mapping theorem to generate the exact many-body ground state. The most fundamental definition of BEC and the condensate orbital is based on the large distance behavior of the one-particle reduced density matrix $\rho_1(x, x')$. If off-diagonal long-range order (ODLRO) is present and hence the largest eigenvalue of ρ_1 is macroscopic (proportional to N) then the system is said to exhibit true BEC and the corresponding eigenfunction, the condensate orbital, plays the role of an order parameter [20,21]. Although the precise definition of ODLRO requires a thermodynamic limit not strictly applicable to mesoscopic traps, the GP approximation

assumes from the start that ODLRO and macroscopic occupation of a single orbital are good approximations in a trap, so examination of this assumption in the Olshanii limit [8] is important. In the remainder of this paper we shall determine the many-body ground state and its salient features, including the one-particle reduced density matrix and its eigenvalues (occupation number distribution function) and eigenfunctions (natural orbitals), as well as the momentum distribution function.

II. EXACT GROUND STATE WAVE FUNCTION

The Hamiltonian of N bosons in a 1D harmonic trap is

$$\hat{H} = \sum_{j=1}^N \left[-\frac{\hbar^2}{2m} \frac{\partial^2}{\partial x_j^2} + \frac{1}{2} m \omega^2 x_j^2 \right]. \quad (1)$$

We assume that the two-body interaction potential consists only of a hard core of 1D diameter a . This is conveniently treated as a constraint on allowed wave functions $\psi(x_1, \dots, x_N)$ such that

$$\psi = 0 \quad \text{if} \quad |x_j - x_k| < a \quad , \quad 1 \leq j < k \leq N, \quad (2)$$

rather than as an infinite interaction potential. It follows from the Fermi-Bose mapping theorem [10,11,14] that the exact N -boson ground state ψ_{B0} of the Hamiltonian (1) with the constraint (2) is

$$\psi_{B0}(x_1, \dots, x_N) = |\psi_{F0}(x_1, \dots, x_N)|, \quad (3)$$

where ψ_{F0} is the ground state of a fictitious system of N spinless fermions with the same Hamiltonian (1) and constraint. At low densities it is sufficient [8,9] to consider the case of impenetrable point particles, the zero-range limit $a \rightarrow 0$ of (2). Since wave functions of "spinless fermions" are antisymmetric under coordinate exchanges, their wave functions vanish automatically whenever any $x_j = x_k$, the constraint has no effect, and the corresponding fermionic ground state is the ground state of the *ideal* gas of fermions, a Slater determinant of the lowest N single-particle eigenfunctions ϕ_n of the harmonic oscillator (HO)

$$\psi_{F0}(x_1, \dots, x_N) = \frac{1}{\sqrt{N!}} \det_{(n,j)=(0,1)}^{(N-1,N)} \phi_n(x_j). \quad (4)$$

The HO orbitals are

$$\varphi_n(x) = \frac{1}{\pi^{1/4} x_{osc}^{1/2} \sqrt{2^n n!}} e^{-Q^2/2} H_n(Q) \quad (5)$$

with $H_n(Q)$ the Hermite polynomials and $Q = x/x_{osc}$, $x_{osc} = \sqrt{\hbar/m\omega}$ being the ground state width of the harmonic trap for a single atom. By factoring the Gaussians out of the determinant and carrying out elementary row and column operations, one can cancel all terms in each H_n except the one of highest degree, with the result [22]

$$\begin{aligned}
\det_{(n,j)=(0,1)}^{(N-1,N)} H_n(x_j) &= 2^{N(N-1)/2} \det_{(n,j)=(0,1)}^{(N-1,N)} (x_j)^n \\
&= 2^{N(N-1)/2} \prod_{1 \leq j < k \leq N} (x_k - x_j)
\end{aligned} \tag{6}$$

Substitution into (3) then yields a simple but exact analytical expression of Bijl-Jastrow pair product form for the N -boson ground state:

$$\psi_{B0}(x_1, \dots, x_N) = C_N \left[\prod_{i=1}^N e^{-Q_i^2/2} \right] \prod_{1 \leq j < k \leq N} |x_k - x_j| \tag{7}$$

with $Q_i = x_i/x_{osc}$ and normalization constant

$$C_N = 2^{N(N-1)/4} \left(\frac{1}{x_{osc}} \right)^{N/2} \left[N! \prod_{n=0}^{N-1} n! \sqrt{\pi} \right]^{-1/2}. \tag{8}$$

It is interesting to note the strong similarity between this exact 1D N -boson wave function and the famous Laughlin variational wave function of the 2D ground state for the quantized fractional Hall effect [23], as well as the closely-related wave functions for bosons with weak repulsive delta-function interactions in a harmonic trap in 2D found recently by Smith and Wilkin [24].

III. GROUND STATE PROPERTIES

In this section we numerically evaluate the ground state properties of a 1D condensate of N hard core bosons in a harmonic trap using the exact many-body wave function of the previous section.

A. Single particle density and pair distribution function

Both the single particle density and pair distribution function depend only on the absolute square of the many-body wave function, and since $|\psi_{B0}|^2 = |\psi_{F0}|^2$ they reduce to standard ideal Fermi gas expressions. The single particle density, normalized to N , is

$$\begin{aligned}
\rho(x) &= N \int |\psi_{B0}(x, x_2, \dots, x_N)|^2 dx_2 \cdots dx_N \\
&= \sum_{n=0}^{N-1} |\varphi_n(x)|^2
\end{aligned} \tag{9}$$

We shall not exhibit it here since it has recently been calculated by Kolomeisky *et al.* [16]; see also our recent discussion of the time-dependent case [17]. The pair distribution function, normalized to $N(N-1)$, is

$$\begin{aligned}
D(x_1, x_2) &= N(N-1) \int |\psi_{B0}(x_1, \dots, x_N)|^2 dx_3 \cdots dx_N \\
&= \sum_{0 \leq n < n' \leq N-1} |\varphi_n(x_1)\varphi_{n'}(x_2) - \varphi_n(x_2)\varphi_{n'}(x_1)|^2
\end{aligned} \tag{10}$$

Physically, the pair distribution function is the joint probability density that if one atom is measured at x_1 then a second measurement immediately following the first finds an atom at x_2 . Noting that terms with $n = n'$, which vanish by antisymmetry, can be formally added to the summation (9), one can rewrite the pair distribution function in terms of the single particle density and a correlation function Δ :

$$D(x_1, x_2) = \rho(x_1)\rho(x_2) - |\Delta(x_1, x_2)|^2$$

$$\Delta(x_1, x_2) = \sum_{n=0}^{N-1} \varphi_n^*(x_1)\varphi_n(x_2) \quad (11)$$

Although the Hermite polynomials have disappeared from the expression (7) for the many-body wave function, they reappear upon integrating $|\psi_{B0}|^2$ over $(N - 1)$ coordinates to get the single particle density $\rho(x)$ and over $(N - 2)$ to get the pair distribution function $D(x_1, x_2)$, and the expressions in terms of the HO orbitals φ_n are the most convenient for evaluation.

Figure 1 shows a gray scale plot of the dimensionless pair distribution function $x_{osc}^2 \cdot D(Q_1, Q_2)$ versus the normalized coordinates $Q_{1,2} = x_{1,2}/x_{osc}$ for a) $N = 2$, b) $N = 6$, and c) $N = 10$. Some qualitative features of the pair distribution function are apparent: In the first place it follows either from the original expression (9) or from Eqs. (8) and (10) that $D(x_1, x_2)$ vanishes at contact $x_1 = x_2$, as it must because of impenetrability of the particles, and we see this to be true in Fig. 1. Furthermore, the correlation term $\Delta(x_1, x_2)$ is a truncated closure sum and approaches the Dirac delta function $\delta(x_1 - x_2)$ as $N \rightarrow \infty$, as is to be expected since the healing length in a spatially uniform 1D hard core Bose gas varies inversely with particle number [14]. As a result the width of the null around the diagonal $Q_1 = Q_2$ decreases with increasing N , and vanishes in the limit. Away from the diagonal along $Q_2 = -Q_1$ the pair distribution function rises, exhibits modulations for $N > 2$, due to the oscillatory nature of the HO orbitals, before decreasing back to zero at large distances. For $|x_1 - x_2|$ much larger than the healing length, D reduces to the uncorrelated density product $\rho(x_1)\rho(x_2)$, so the spatial extent of the pair distribution function is that of the density and varies as $N^{1/2}$ [16].

B. Reduced single-particle density matrix

The reduced single-particle density matrix with normalization $\int \rho_1(x, x)dx = N$ is given by

$$\begin{aligned} \rho_1(x, x') &= N \int \psi_{B0}(x, x_2, \dots, x_N) \\ &\times \psi_{B0}(x', x_2, \dots, x_N) dx_2 \dots dx_N \\ &= \mathcal{N}_N e^{-Q^2/2} e^{-(Q')^2/2} \int \prod_{i=2}^N e^{-Q_i^2} |Q_i - Q| |Q_i - Q'| \\ &\times \left[\prod_{2 \leq j < k \leq N} (Q_k - Q_j)^2 \right] dQ_2 \dots dQ_N, \end{aligned} \quad (12)$$

with

$$\mathcal{N}_N = N \cdot 2^{N(N-1)/2} x_{osc}^{-1} \left[N! \prod_{n=0}^{N-1} n! \sqrt{\pi} \right]^{-1}. \quad (13)$$

Although the multi-dimensional integral (12) cannot be evaluated analytically, it can be evaluated numerically by Monte Carlo integration for not too large values of N (the computing time scales as N^4). Figure 2 shows a gray scale plot of the dimensionless reduced single-particle density matrix $x_{osc} \cdot \rho_1(Q, Q')$ versus the normalized coordinates Q and Q' for a) $N = 2$, b) $N = 6$, and c) $N = 10$. We verified that along the diagonal $\rho_1(Q, Q' = Q) = \rho(Q)$ reproduced the single-particle density [16]. The off-diagonal elements of the reduced density matrix relate to ODLRO, and it is clear that as N increases the off-diagonal elements are decreasing in contrast to the diagonal. This is a first indication that ODLRO vanishes for a system of hard core bosons in a 1D HO in the thermodynamic limit.

C. ODLRO, natural orbitals and their occupation

In a macroscopic system, the presence or absence of BEC is determined by the behavior of $\rho_1(x, x')$ as $|x - x'| \rightarrow \infty$. Off-diagonal long-range order is present if the largest eigenvalue of ρ_1 is macroscopic (proportional to N), in which case the system exhibits BEC and the corresponding eigenfunction, the condensate orbital, plays the role of an order parameter [20,21]. Although this criterion is not strictly applicable to mesoscopic systems, if the largest eigenvalue of ρ_1 is much larger than one then it is reasonable to expect that the system will exhibit some BEC-like coherence effects. Thus we examine here the spectrum of eigenvalues λ_j and associated eigenfunctions $\phi_j(x)$ (“natural orbitals”) of ρ_1 . Although natural orbitals are a much-used tool in theoretical chemistry, they have only recently been applied to mesoscopic atomic condensates [25]. The relevant eigensystem equation is

$$\int_{-\infty}^{\infty} \rho_1(x, x') \phi_j(x') dx' = \lambda_j \phi_j(x) \quad (14)$$

λ_j represents the occupation of the orbital ϕ_j , and one has $\sum_j \lambda_j = N$. Numerical evaluation of the integral (13) by discretization yields a readily-solved matrix eigensystem equation which yields accurate numerical results for the largest eigenvalues and associated eigenvectors. In Fig. 3(a) we show a log-log plot of the fractional occupation of the lowest orbital $f_0 = \lambda_0/N$ versus the total particle number N (solid line), along with a best fit power-law $f_0 \approx N^{-0.41}$ (dashed line). This is to be contrasted with the case of a spatially uniform system of hard core bosons for which $f_0 \approx N^{-0.5}$ [12]. In both cases the fractional occupation decreases with increasing N , and thus do not correspond to true condensates for which $f_0 = 1$. Nevertheless, the occupation of the lowest orbital may still be large $\lambda_0 \approx N^{0.59}$, and is larger than the spatially uniform case $\lambda_0 \approx N^{0.5}$, so macroscopic quantum coherence effects reminiscent of BEC can still result [8,12–14,16,17].

Figure 3(b) shows the distribution of occupations λ_j versus orbital number j (the orbitals are ordered according to eigenvalue magnitude, the largest eigenvalue being $j = 0$) for $N = 2$ (circles), $N = 6$ (stars), and $N = 10$ (squares). This figure shows that as the lowest orbital occupation λ_0 increases with increasing N so does the range of significantly occupied higher-order orbitals with $j > 0$. This means that the dominance of the lowest orbital decreases

with increasing N , so singling out $\phi_0(x)$ as a macroscopic wave function for the whole system becomes more problematic with increasing N [17,16].

The numerically computed lowest orbitals $\phi_0(Q)$ are shown in Fig 4 for a) $N = 2$, b) $N = 6$, and c) $N = 10$, and they show the expected broadening due to many-body repulsion as N increases. We remark that these lowest orbitals are not simply the square root of the corresponding single-particle densities $\rho(Q)$ [16] as would be the case for a true condensate. Figure 5 shows the higher order orbitals $\phi_j(Q)$ versus Q for $j = 1, 2, 3$ and $N = 10$. Although the higher-order orbitals differ in detail from the HO orbitals they share the features that the orbitals can be chosen real by removal of an overall phase, and that the j^{th} orbital has j zeros.

IV. MOMENTUM DISTRIBUTION

For a spatially uniform system (no trap) the natural orbitals are plane waves, so the occupation distribution of the natural orbitals is the same as the momentum distribution. Although this is not the case here due to the effect of the harmonic trap potential, the momentum distribution is still physically important, so we study it here. In terms of the boson annihilation and creation operators in position representation (quantized Bose field operators) the one-particle reduced density matrix is

$$\rho_1(x, x') = \langle \Psi_{B0} | \hat{\psi}^\dagger(x') \hat{\psi}(x) | \Psi_{B0} \rangle \quad (15)$$

The momentum distribution function $n(k)$, normalized to $\int_{-\infty}^{\infty} n(k) dk = N$, is $n(k) = \langle \Psi_{B0} | \hat{a}^\dagger(k) \hat{a}(k) | \Psi_{B0} \rangle$ where $\hat{a}(k)$ is the annihilation operator for a boson with momentum $\hbar k$. Then

$$n(k) = (2\pi)^{-1} \int_{-\infty}^{\infty} dx \int_{-\infty}^{\infty} dx' \rho_1(x, x') e^{-ik(x-x')} \quad (16)$$

The spectral representation of the density matrix then leads to $n(k) = \sum_j \lambda_j |\mu_j(k)|^2$ where the μ_j are Fourier transforms of the natural orbitals: $\mu_j(k) = (2\pi)^{-1/2} \int_{-\infty}^{\infty} \phi_n(x) e^{-ikx} dx$. Figure 6 shows the numerically calculated dimensionless momentum spectrum $k_{osc} \cdot n(\kappa)$ versus normalized momentum $\kappa = k/k_{osc}$, with $k_{osc} = 2\pi/x_{osc}$, for a) $N = 2$, b) $N = 6$, and c) $N = 10$. The key features are that the momentum spectrum maintains the sharp peaked structure reminiscent of the spatially uniform case [8,12] for the 1D HO, and that the peak becomes sharper with increasing atom number N . This is to be expected since as the number of atoms increase the many-body repulsion causes the system to become more spatially uniform within the trap interior.

V. SUMMARY AND CONCLUSIONS

In summary, we have investigated the ground state properties of a system of hard core bosons in a 1D HO using the exact many-body wave function obtained using the Fermi-Bose mapping theorem. Specifically, we have numerically evaluated the reduced single-particle density matrix for the system using Monte-Carlo integration for particle numbers up to $N = 10$, and extracted several quantities of physical significance, including the natural

orbitals and momentum spectrum. Our main finding is that the lowest orbital occupation scales as $\lambda_0 \approx N^{0.59}$, so that the system does not exhibit true BEC, counter to the case of an ideal gas in a 1D HO [19]. Furthermore, this makes the introduction of an order-parameter or macroscopic wave function for the whole system more problematic for large N . We have started to seek analytic approaches to derive the observed scaling of the lowest orbital with particle with no success so far. We hope that these numerical results may motivate others to approach this challenging problem.

This work was supported by Office of Naval Research grant N00014-99-1-0806.

REFERENCES

- [1] M. Key *et al.*, *Phys. Rev. Lett.* **84**, 1371 (2000).
- [2] D. Müller *et al.*, *Phys. Rev. Lett.* **83**, 5194 (1999).
- [3] N.H. Dekker *et al.*, *Phys. Rev. Lett.* **84**, 1124 (2000).
- [4] J.H. Thywissen, R.M. Westervelt, and M. Prentiss, *Phys. Rev. Lett.* **83**, 3762 (1999).
- [5] E.A. Hinds, M.G. Boshier, and I.G. Hughes, *Phys. Rev. Lett.* **80**, 645 (1998).
- [6] *Atom Interferometry*, ed. P.R. Berman (Academic Press, Boston, 1997).
- [7] J. Schmiedmayer, *Eur. Phys. J. D* **4**, 57 (1998).
- [8] M. Olshanii, *Phys. Rev. Lett.* **81**, 938 (1998).
- [9] D. S. Petrov, G. V. Shlyapnikov, and J. T. M. Walraven, "Regimes of quantum degeneracy in trapped 1D gases," cond-mat/0006339 (2000).
- [10] M. Girardeau, *J. Math. Phys.* **1**, 516 (1960).
- [11] M.D. Girardeau, *Phys. Rev.* **139**, B500 (1965). See particularly Secs. 2, 3, and 6.
- [12] A. Lenard, *J. Math. Phys.* **7**, 1268 (1966).
- [13] A. G. Rojo, G. L. Cohen, and P. R. Berman, *Phys. Rev. A* **60**, 1482 (1999).
- [14] M.D. Girardeau and E.M. Wright, *Phys. Rev. Lett.* **84**, 5691 (2000).
- [15] K. Bongs *et al.*, "A waveguide for Bose-Einstein condensates," cond-mat/0007381 (2000).
- [16] E. B. Kolomeisky *et al.* *Phys. Rev. Lett.* **85**, 1146 (2000).
- [17] M.D. Girardeau and E.M. Wright, *Phys. Rev. Lett.* **84**, 5239 (2000).
- [18] H.G. Vaidya and C.A. Tracey, *Phys. Rev. Lett.* **42**, 3 (1979).
- [19] W. Ketterle and N. J. Van Druten, *Phys. Rev. A* **54**, 656 (1996).
- [20] O. Penrose and L. Onsager, *Phys. Rev.* **104**, 576 (1956).
- [21] C.N. Yang, *Rev. Mod. Phys.* **34**, 694 (1962).
- [22] A.C. Aitken, *Determinants and Matrices* (Oliver and Boyd, Edinburgh and London, 1951), p. 112.
- [23] R.B. Laughlin, *Phys. Rev. Lett.* **50**, 1395 (1983).
- [24] R.A. Smith and N.K. Wilkin, "Exact eigenstates for repulsive bosons in two dimensions," cond-mat/0005230 (2000).
- [25] J. L. DuBois and H. R. Glyde, "Bose-Einstein condensation in trapped bosons: A variational Monte Carlo analysis," cond-mat/0008368 (2000).

FIGURES

FIG. 1. Gray-scale plots of the dimensionless pair distribution function $x_{osc}^2 \cdot D(Q_1, Q_2)$ as a function of the dimensionless coordinates Q_1 and Q_2 , for a) $N = 2$, b) $N = 6$, and c) $N = 10$.

FIG. 2. Gray-scale plots of the dimensionless reduced density matrix $x_{osc} \cdot \rho_1(Q, Q')$ as a function of the dimensionless coordinates Q and Q' , for a) $N = 2$, b) $N = 6$, and c) $N = 10$.

FIG. 3. Occupation of the natural orbitals: a) fraction of atoms in the lowest orbital $f_0 = \lambda_0/N$ versus N , and b) λ_j versus orbital number j for $N = 2$ (circles), $N = 6$ (stars), and $N = 10$ (squares).

FIG. 4. Lowest natural orbitals $\phi_0(Q)$ versus normalized coordinate Q for a) $N = 2$, b) $N = 6$, and c) $N = 10$.

FIG. 5. Higher-order natural orbits $\phi_j(Q)$ versus normalized coordinate Q for $N = 10$ and a) $j = 1$, b) $j = 2$, and c) $j = 3$.

FIG. 6. Dimensionless momentum distribution $k_{osc} \cdot n(\kappa)$ versus normalized momentum $\kappa = k/k_{osc}$ for a) $N = 2$, b) $N = 6$, and c) $N = 10$.

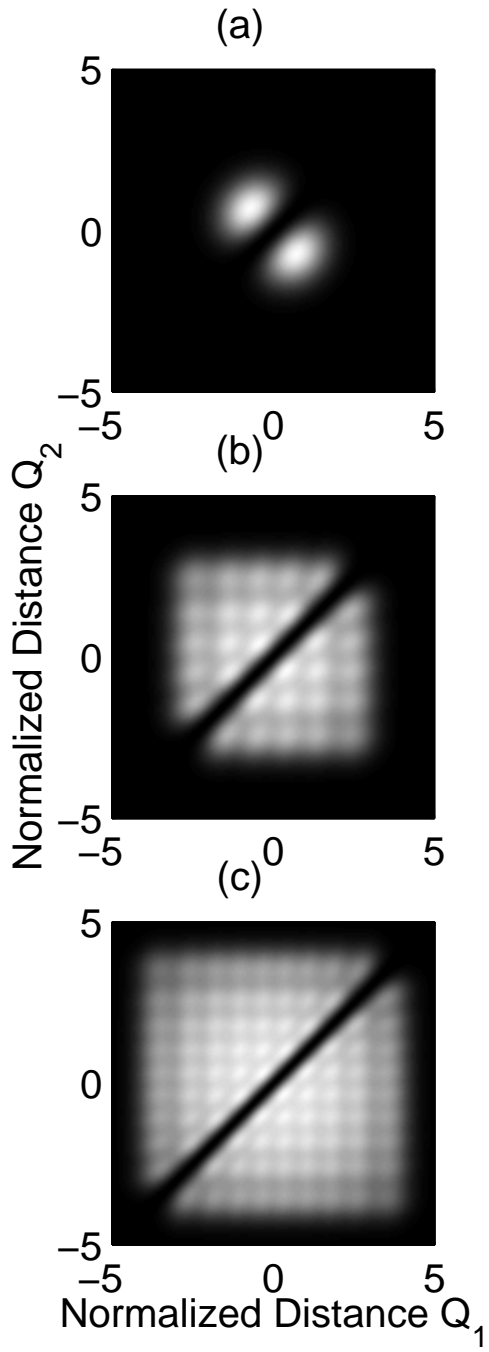


Figure 1

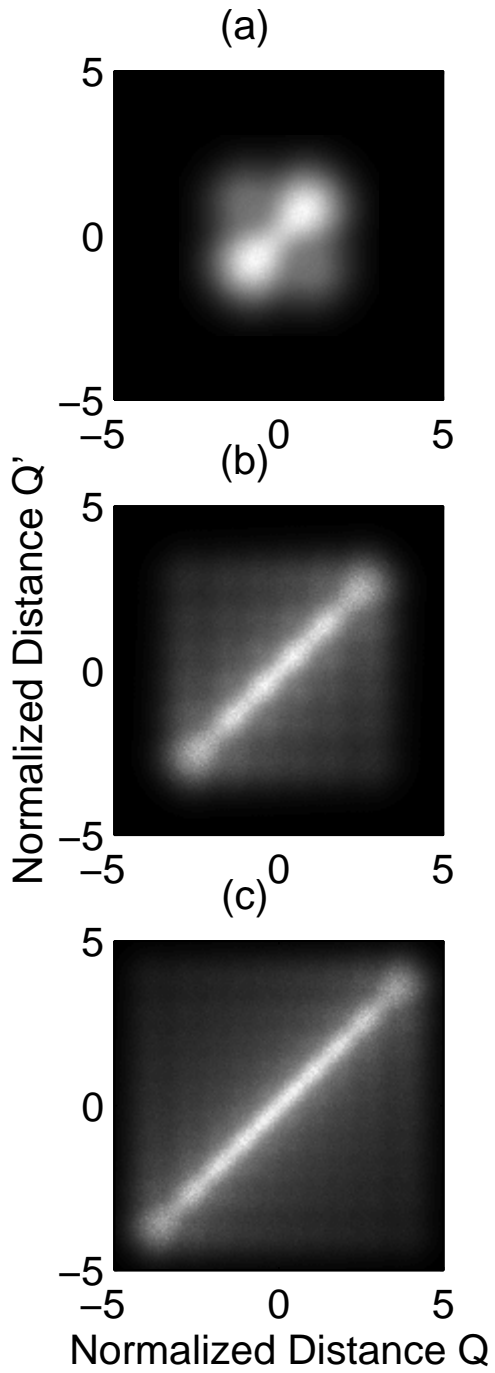


Figure 2

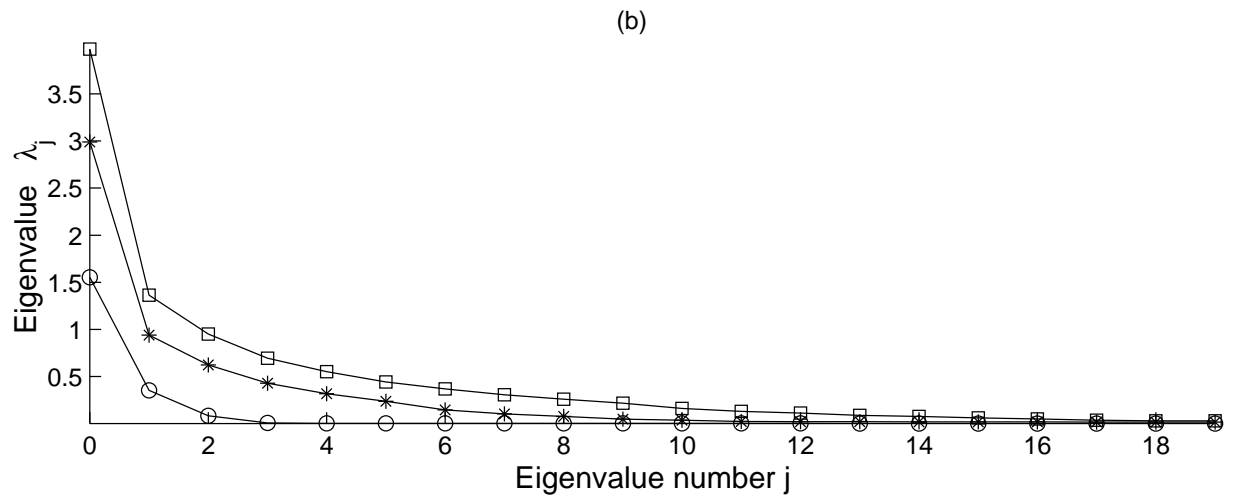
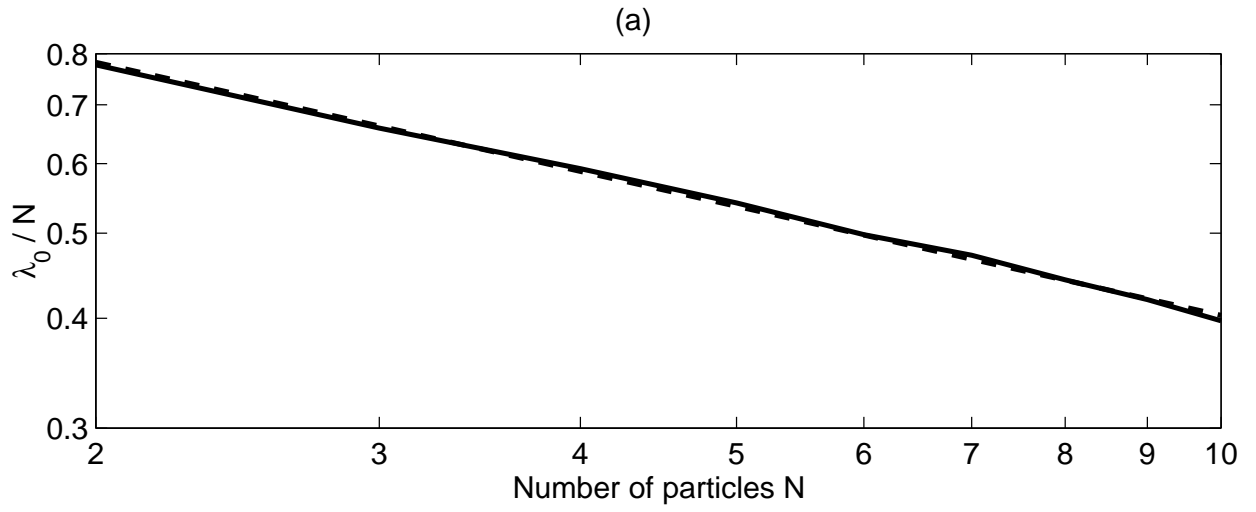


Figure 3

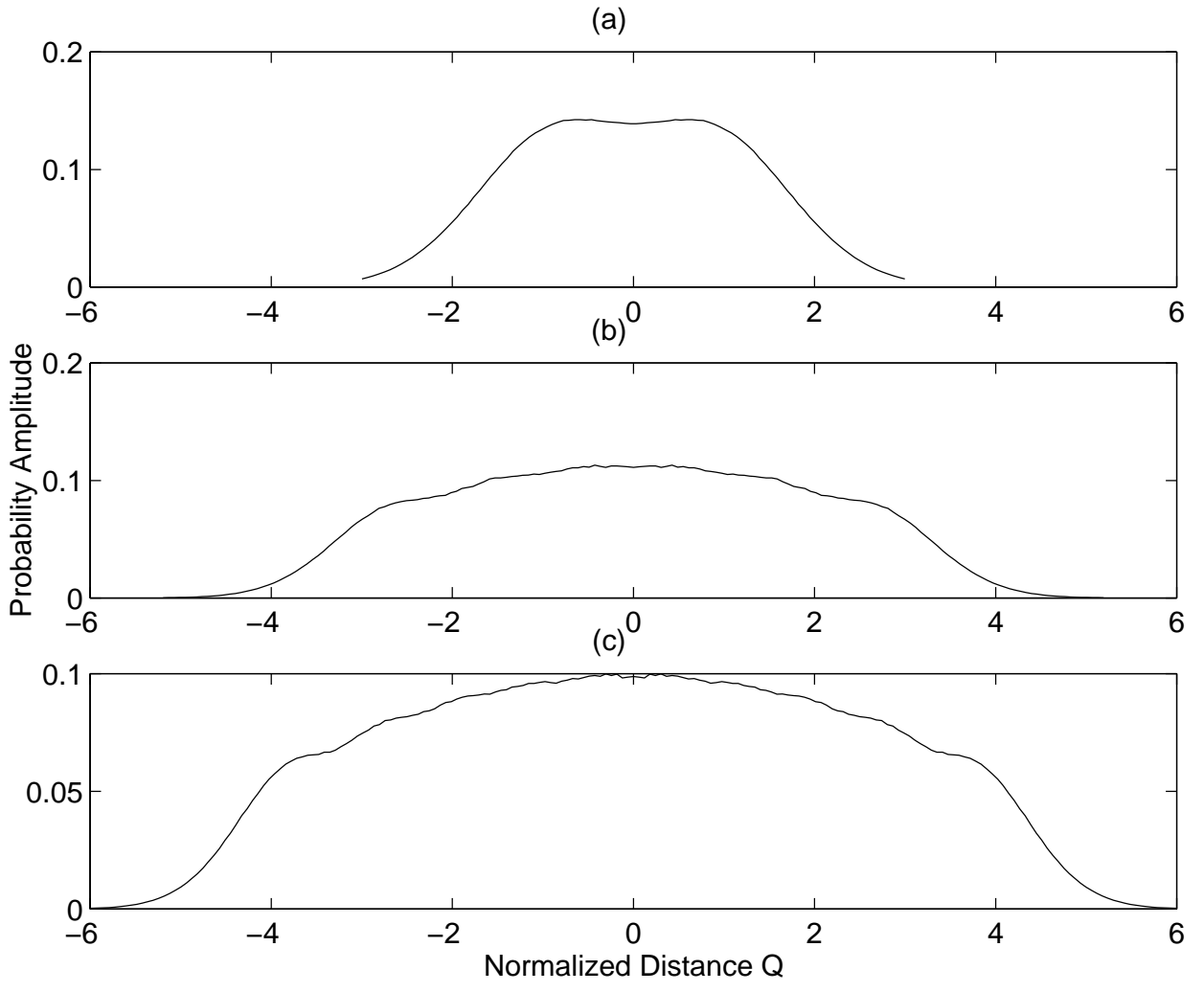


Figure 4

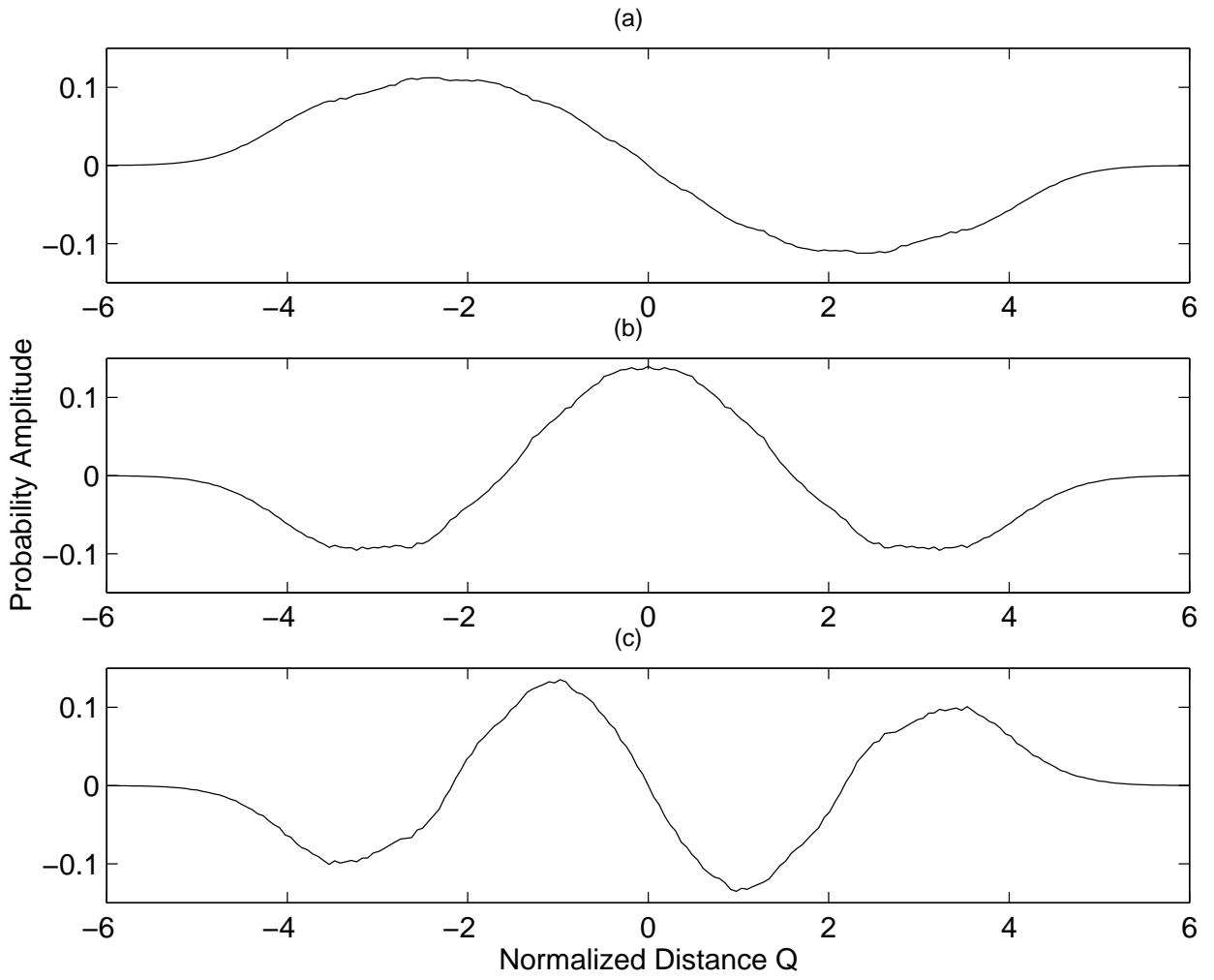


Figure 5

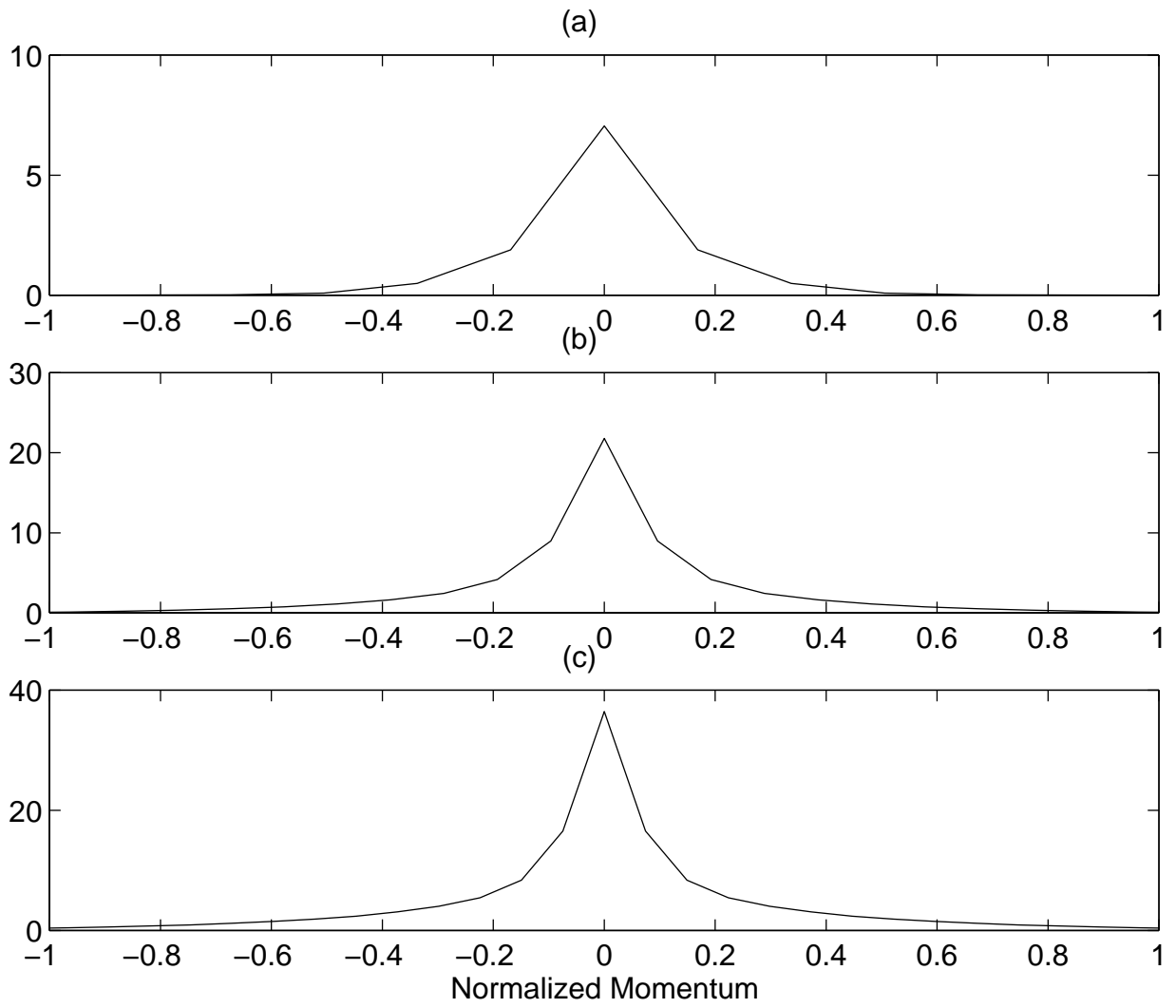


Figure 6